



10th International Meeting on Thermodiffusion

## Thermodiffusion in ferrofluids regarding thermomagnetic convection

Lisa Sprenger\*, Adrian Lange, Stefan Odenbach

Technische Universität Dresden, Institute of Fluid Mechanics, Chair of Magnetofluidynamics, 01062 Dresden, Germany

## ARTICLE INFO

## Article history:

Available online 15 March 2013

## Keywords:

Ferrofluids  
 Magnetic fluids  
 Rayleigh number  
 Soret coefficient  
 Thermodiffusion  
 Thermomagnetic convection

## ABSTRACT

Magnetic fluids, also called ferrofluids, are binary liquids consisting of magnetic nanoparticles being dispersed in a carrier liquid. They show very strong thermodiffusive behaviour with a Soret coefficient ( $S_T$ ) of approximately  $0.16 \text{ K}^{-1}$  without a magnetic field. The dependence of the Soret coefficient on a magnetic field can lead to even higher values, and to a change in the coefficient's sign. This change in the direction of movement of the nanoparticles strongly affects the onset of thermomagnetic convection. A linear stability analysis reveals that thermodiffusion with a positive sign of the Soret coefficient enhances the onset of convection, whereas negative coefficients starting at about  $-0.001 \text{ K}^{-1}$  suppress convection at all.

© 2013 Académie des sciences. Published by Elsevier Masson SAS. All rights reserved.

## 1. Introduction

Magnetic fluids are usually composed of magnetite or cobalt nanoparticles dispersed in a carrier liquid such as kerosene, oil or water. The particles have diameters close to 10 nm, and are coated with a surfactant layer of about 2 nm [1,2]. The surfactant is needed to keep the particles stably dispersed, and is matched with the specific carrier fluid. In the case of a zero magnetic field, the fluid does not behave magnetically, since the magnetic moments of the single-domain particles are distributed stochastically. When the fluid is exposed to an external magnetic field, these magnetic moments align with the field direction so that the fluid becomes magnetised. This behaviour is called super-paramagnetic, and is characterised by the magnetisation curve indicating the dependence of the magnetisation on the strength of the magnetic field [1,2]. This curve can be measured experimentally and provides characteristic values of the magnetic fluid such as the average magnetic diameter of the particles, the saturation magnetisation, and the volume concentration derived from the latter.

Thermomagnetic convection in that context denotes a transport phenomenon driven by a spatially varying magnetisation in a layer of a magnetic fluid. A vertical variation is caused by a temperature difference applied to the upper and lower boundaries of the layer. The occurring gradient in the magnetisation results in a gradient in the internal magnetic field of the fluid. A small perturbation in the fluid such as the adiabatic dislocation of a volume element then leads to a difference in the magnetisation of the dislocated element with its surrounding. This difference interacts with the internal magnetic field gradient and the resulting force is directed in favour of the direction of the initial perturbation [3–7]. Measurements [6,7] have been carried out with the aim to determine the critical temperature difference needed at fixed magnetic field strengths to start convection in a layer of ferrofluid. The onset is detected by measuring the heat flux over the layer's upper boundary. A change in the mechanism of heat transport from conductive to convective yields an enhanced flux [4–6]. At field strength of 25 kA/m and a parallel orientation of the magnetic field to the temperature difference, convection sets in at a lower critical temperature difference than in the zero field case for an oil-based ferrofluid [6]. Therefore, it is assumed that the magnetic field enhances convection. In the same setup using a kerosene-based ferrofluid, suppression of convection

\* Corresponding author.

E-mail address: [Lisa.Sprenger@tu-dresden.de](mailto:Lisa.Sprenger@tu-dresden.de) (L. Sprenger).

was detected [7]. Since fluid parameters such as viscosity are not notably dependent on the magnetic field for both tested fluids, one has to find a temperature-driven transport process opposing the convective motion in one case and enhancing it in the other.

Such a transport process can be thermodiffusion, which is driven by a temperature gradient, causing a movement of the particles of a binary liquid either to the warmer side of the layer, characterised by a negative Soret coefficient or to the colder side, indicated by a positive Soret coefficient. Measurements of the separation process in ferrofluids are usually done by thermogravitational columns [8–10] or horizontal thermodiffusion cells [11]. The concentration gradient established due to the temperature gradient cannot be resolved in detail; the measurement principle is based on determining the average change in concentration of a fluid volume above and below the region of separation [8–11]. While the separation in the thermogravitational column takes place in the horizontal direction, supported by convection [8–10], the separation direction in the thermodiffusion cell is vertical and convection is absent [11]. The detection of the concentration in the fluid volumes is done by sensor coils. Their inductance is sensitive to the amount of magnetic material inside. A basic design for a horizontal cell was used by [11] to perform the first magnetic-field-dependent Soret coefficient experiments. Using a kerosene-based ferrofluid with a volume concentration of 2% of magnetite particles [11], a positive Soret coefficient was detected for the case when the magnetic field is aligned perpendicular to the temperature gradient. The magnitude of the coefficient was slightly above the non-magnetic value of  $0.16 \text{ K}^{-1}$ . Orienting the magnetic field parallel to the temperature difference, a negative Soret coefficient was measured [11]. For the strongest tested magnetic field, its absolute value of  $|-0.6| \text{ K}^{-1}$  was four times higher than the non-magnetic value. A shift from a positive Soret to a negative Soret coefficient took place at field strength of about 25 kA/m [11].

The general interaction between thermodiffusion and convection in ferrofluids has already been proofed experimentally in zero magnetic field in [12]. Therefore, further investigations on that subject including magnetic fields as described in the following are of high interest.

## 2. Thermomagnetic convection

### 2.1. Governing equations

As setup for the investigation of thermomagnetic convection, a horizontal layer of ferrofluid with a vertical thickness  $h$  is considered. The layer is bounded by impermeable walls at  $z = \pm h/2$ , and the fluid is regarded as incompressible with  $\rho$  being its density, and  $\nu(\eta)$  its kinematic (dynamic) viscosity. The equations describing this system are based on the balance equations of mass, momentum, heat, and concentration, and additionally on the Maxwell equations for the magnetic field strength  $\underline{H}$  and flux  $\underline{B}$ . The dimensionless equations in the Boussinesq approximation [13,14] then read:

$$\text{div}(\underline{v}) = 0 \tag{1}$$

$$\partial \underline{v} / \partial t + \underline{v} \text{grad}(\underline{v}) = -\text{grad}(p) + Ra Pr((T - T_0) - \Psi(C - C_0)) + Ra_m Pr \text{grad}(\underline{H}\underline{B}) + Pr \Delta \underline{v} \tag{2}$$

$$\partial T / \partial t = \Delta T \tag{3}$$

$$\partial C / \partial t = Le_m(\Delta C + \Delta T) \tag{4}$$

$$\text{div}(\underline{B}) = 0 \tag{5}$$

$$\text{rot}(\underline{H}) = 0 \tag{6}$$

where the temperature  $T$  is scaled by  $\Delta T$ , the temperature difference between the two boundary layers, the concentration  $C$  by  $\Delta T k_{T_m} / T_0$ , the velocity  $\underline{v}$  by  $\kappa / h$ , all lengths by  $h$ , the time  $t$  by  $h^2 / \kappa$ , the pressure  $p$  by  $\kappa^2 \rho / h^2$ , the magnetic field by  $K \Delta T$ , and the magnetic flux by  $\mu_0 K \Delta T$ .  $K$  denotes the pyromagnetic coefficient,  $\kappa$  is the heat coefficient,  $Le_m = D_m / \kappa$  is the magnetic Lewis number, with  $D_m$  being the magnetic molecular diffusion coefficient, while  $k_{T_m} = S_T T_0 C_0 (1 - C_0)$ .  $C_0$  is the dimensionless initial mass concentration of the nanoparticles in the fluid,  $T_0$  the dimensionless initial homogeneous temperature. The coefficient  $\Psi$  is called separation rate and is defined by  $S_T \beta_C / \beta_T$ . The Rayleigh number  $Ra$  is defined as  $(\beta_T g h^3 \Delta T) / (\kappa \nu)$ , with  $\beta_T$  being  $-1 / \rho_0 \partial \rho / \partial T$ . The Prandtl number  $Pr$  denotes  $\nu / \kappa$ . The magnetic Rayleigh number  $Ra_m$  reads  $(\mu_0 K^2 \Delta T^2 h^2) / (\kappa \eta)$ . The equations of state for the density  $\rho = \rho_0 (1 - \beta_T (T - T_0) + \beta_C (C - C_0))$ , with  $\beta_C = 1 / \rho_0 \partial \rho / \partial C$ , and the magnetisation  $M = M_0 + \partial M / \partial T (T - T_0) + \partial M / \partial C (C - C_0)$  complement the hydrodynamic and magnetic equations.

The system of equations is finally completed by the boundary conditions. There are the no-slip condition for the velocity, the condition of fixed temperatures at the walls and the impermeability for the mass flux:

$$\underline{v}|_{z=\pm 0.5} = \underline{0} \tag{7}$$

$$T|_{z=-0.5} = T_0 + 0.5, \quad T|_{z=+0.5} = T_0 - 0.5 \tag{8}$$

$$(\partial_z C + \partial_z T)|_{z=\pm 0.5} = 0 \tag{9}$$

The boundary condition for the magnetic field demands equality of the tangential components on both sides of the horizontal boundaries, whereas in the case of the magnetic flux, equality of the normal component is claimed. This system of equations is used for the linear stability analysis, described in the following.

## 2.2. Linear stability analysis

For carrying out a linear stability analysis of the system described above, the ground state of this system has to be known. It is characterised by a fluid at rest, a linear temperature gradient, and usually by the conductive state of the concentration. But since the concentration profile establishes much slower than the temperature gradient, the concentration is regarded as constant, using the initial homogeneous concentration  $C_0$ , according to [14]. Eqs. (10) to (12) represent the ground state:

$$\underline{v} = \underline{0} \quad (10)$$

$$T = T_0 - z \quad (11)$$

$$C = C_0 \quad (12)$$

In the next step, small deviations from the ground state are considered. They are named  $\Theta$ ,  $\delta c$ ,  $\phi$ , and  $\underline{v}$  and  $w$  for the temperature, the concentration, the magnetic field potential, and the velocity itself and its  $z$ -component. After linearising with respect to these deviations, the system looks like:

$$\text{div}(\underline{v}) = \underline{0} \quad (13)$$

$$\begin{aligned} \partial/\partial t \Delta w = Ra Pr ((\partial_{xx} + \partial_{yy})\Theta - \Psi(\partial_{xx} + \partial_{yy})\delta c) \\ - Ra_m Pr / (1 + \chi)(\partial_{xx} + \partial_{yy})(\partial_z \phi / (1 + \chi) - \Theta + \partial M / \partial C \delta c) + Pr \Delta \Delta w \end{aligned} \quad (14)$$

$$\partial \Theta / \partial t - w = \Delta \Theta \quad (15)$$

$$\partial \delta c / \partial t = Le_m (\Delta \delta c + \Delta \Theta) \quad (16)$$

$$\text{div}(\underline{B}) = 0 \quad (17)$$

with the free boundary conditions reading:

$$\partial_{zz} w = w = \Theta = \partial_z \phi = \partial_z \delta c + \partial_z \Theta = 0 \quad (18)$$

In order to express the onset of convection by the Rayleigh number only, it is necessary to substitute the magnetic Rayleigh number by an expression containing the thermal Rayleigh number. Following the suggestion in [3],  $Ra_m$  becomes  $M_1 Ra$ , with  $M_1 = (\mu_0 K^2 \Delta T / h) / [(1 + \chi) g \rho \beta_T]$ . The deviations are assumed to be of an exponential form in  $x$ ,  $y$ , and  $t$ . The ansatz for the  $z$ -dependence is chosen in such a way that the boundary conditions are fulfilled by the perturbed state. In summary the ansatz for the deviations explicitly reads:

$$w, \Theta, \delta c \sim \exp(\lambda t) \exp(ik_x x + ik_y y) \cos(\pi z) \quad (19)$$

$$\phi \sim \exp(\lambda t) \exp(ik_x x + ik_y y) \sin(\pi z) \quad (20)$$

Inserting (19) and (20) into the linearised equations and considering the case of marginal stability, i.e.  $\lambda = 0$ , the solution of the system of equations leads to an analytical expression for the Rayleigh number in dependence on the relevant dimensionless system parameters  $\Psi$ ,  $M_1$ ,  $M_3 = (1 + M_0/H_0)/(1 + \chi)$ , and  $\partial M/\partial C$ :

$$Ra = (\pi^2 + k^2)^3 / [k^2 (1 + \Psi + M_1 (1 + \partial M/\partial C) (1 - \pi^2 / (M_3 k^2 + \pi^2)))] \quad (21)$$

where  $k^2 = (k_x^2 + k_y^2)$  is the square of the wave number. This expression for the Rayleigh number is similar to the one by Finlayson [3]. The explicit relation reads  $Ra_{\text{Fin}} = (\pi^2 + k^2) 3 / [k^2 (1 + M_1 (1 - \pi^2 / (M_3 k^2 + \pi^2)))]$ , the difference can be found in the additional, thermodiffusion-related terms of  $\Psi$ , and  $\partial M/\partial C$ , which are both proportional to the Soret coefficient, the first one by definition, the latter due to scaling.

Eq. (21) can be plotted with respect to  $k^2$  for different Soret coefficients which are chosen on the basis of the coefficients measured by [11] for magnetic fields up to 320 kA/m, see Fig. 1. Since coefficients  $M_1$  and  $M_3$  are functions of the magnetic field, their dependence on the field strength is calculated and integrally averaged over the range from 0 to 320 kA/m. As a result  $M_1$  can be approximated by 0.5,  $M_3$  by 1.1. As can be seen in Fig. 1, Soret coefficients stronger negative than  $-0.001 \text{ K}^{-1}$  lead to exclusively negative Rayleigh numbers, independent of the square of the wave number. Positive Soret coefficients lead to positive Rayleigh numbers in the considered region of  $k^2$ . The onset of convective motion for each Soret coefficient is characterised by the minimum Rayleigh number, also called critical Rayleigh number. Its value for the range of the magnetic Soret coefficient is plotted with respect to  $S_T$  in Fig. 2. High positive Soret coefficients lead to low critical Rayleigh numbers which enhance the onset of thermomagnetic convection. Excluding thermal diffusion by  $S_T = 0$  leads to  $Ra_{\text{crit}} = 554$ . Soret coefficients close to  $-0.001 \text{ K}^{-1}$  result in higher Rayleigh numbers up to 1587, and hence hinder the onset of convection in comparison to the case of no thermal diffusion. Since Soret coefficients stronger negative than  $-0.001 \text{ K}^{-1}$  lead to negative Rayleigh numbers, convection is suppressed in this case.

The Rayleigh number shows a very distinct dependence on the Soret coefficient and especially on its sign. So that thorough experimental investigations on thermal diffusion in magnetic fluids are inevitable.

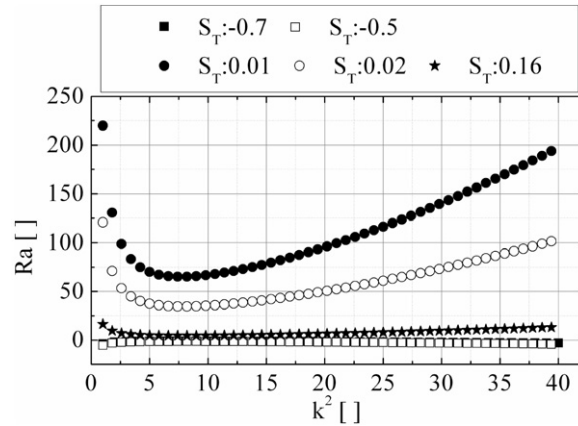


Fig. 1. The Rayleigh number as function of the square of the wave number for different Soret coefficients.

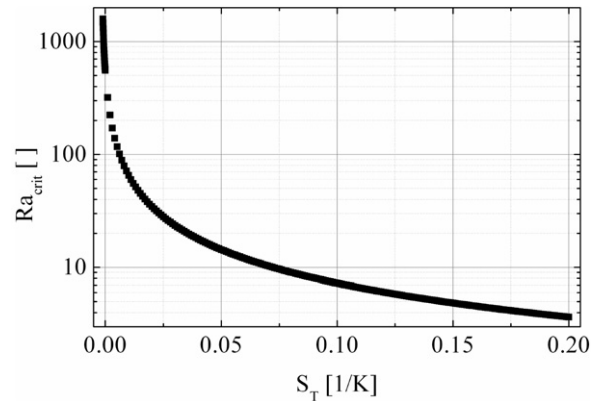


Fig. 2. The critical Rayleigh number versus the Soret coefficient.

### 3. Thermodiffusion

#### 3.1. Experimental setup

In order to investigate the influence of thermodiffusion on the onset of thermomagnetic convection detailed material data concerning the Soret coefficient and its dependence on magnetic field strength and direction is required. The experimental setup has already been described roughly in the introductory part. Fig. 3 gives an overview of the setup. The fluid container, where the actual separation takes place, is denoted by (1), the water baths (2) providing a temperature difference between the upper and lower ends of the cylindrical fluid container. The concentration detection is carried out by the sensor coils (3), wrapped around the fluid cell. Both coils are controlled independently. Fig. 4 shows a close-up of the fluid cell. It is 14 mm high, and a double grid is located in its central part to reduce the effective height for the separation process to 1 mm, which is the distance between the two grids. Additionally, thermomagnetic convection, even possible in a thermally stable setup due to the cell's height, can be excluded in this region [11]. Convection, appearing in the upper or lower container part does not harm the experiment's result, because the sensor coils only detect the average concentration in the whole lower or upper fluid volume.

The detected average values for the magnetic material inside the coils are then used to calculate the Soret coefficient. For that purpose a two-point calibration is always done before starting the actual separation experiment. The empty fluid container is exposed to the temperature gradient. The inductance of the coils is determined over a few hours and then averaged. The cell is then filled with the magnetic fluid and first exposed to the homogeneous initial temperature of 298.15 K. When a stable value for the inductances of the coils is reached, the temperature gradient of 1 K/mm is applied, and registered for about 72 hours. It is assumed that the change in the inductance during the filling process is solely dependent on the concentration of the magnetic nanoparticles in the fluid. Knowing the initial homogeneous concentration enables a correlation between the inductance and the average concentration of the fluid volume.

Measuring the concentration when a magnetic field is applied needs a small adjustment of the measuring process. Since the detection of the concentration of the nanoparticles is done by the magnetic fields of the sensor coils, those fields are three to four orders of magnitude smaller than the external applied field, it is not possible to apply both fields – one for

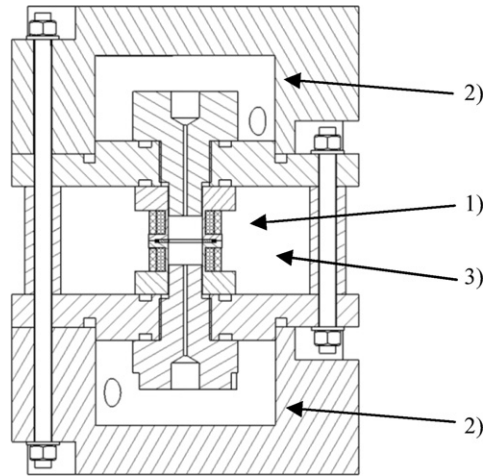


Fig. 3. Horizontal thermodiffusion cell, (1) fluid container, (2) tempering water baths, (3) magnetic-nanoparticle-sensitive sensor coils.

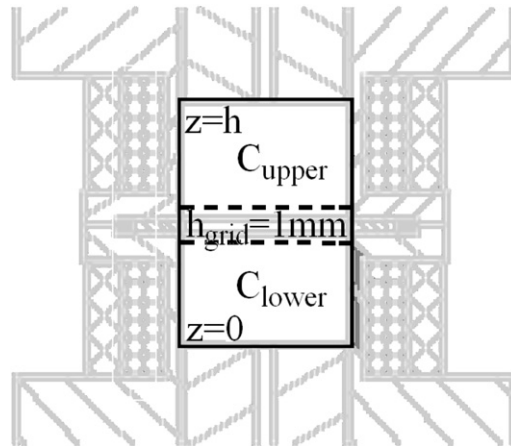


Fig. 4. Close-up of the fluid container, separated centrally by a double layer grid hindering convection to arise in the cell part where the separation takes place.

the detection, one for the separation process – at the same time. This is why approximately every three hours the external magnetic field is shut off in order to measure the concentration for about 10 minutes. The averaged inductance value of these 10 minutes is used for the determination of the concentration at that point in time.

The separation is given by:

$$(C_{lo} - C_{up})/C_0 = 4/(h - h_{grid})S_T D \Delta T / ht \tag{22}$$

according to [11], with  $C_{lo}$ , and  $C_{up}$  denoting the lower and upper concentration in the fluid chambers, and  $h_{grid}$  denotes the height of the double-layer grid (Fig. 4). The concentration difference is thereby measured, the temperature difference as well as the geometric factor are known, and the molecular diffusion coefficient  $D$  can be calculated by the Batchelor-corrected Einstein relation [15], see Eq. (26). This so-called separation curve (22) is based on the assumption that separation only takes place between the two centrally placed grids. Due to the small height of 1 mm a stationary separation state is established rather fast and a constant concentration gradient can be assumed. Solving the description of the concentration profile in space and time for dilute binary fluids:

$$\partial C / \partial t = D \operatorname{div}(\operatorname{grad}(C) + S_T C \operatorname{grad}(T)) \tag{23}$$

and additionally assuming that  $\Delta C$  is much smaller than  $\operatorname{grad}(C)$  and neglecting it for that reason leads to two different expressions for the concentration at the grid boundaries, namely  $C_{lo} = C_{lo}(t)$  and  $C_{up} = C_{up}(t)$ . The subtraction of these two functions results in Eq. (22), then being used to determine the Soret coefficient from measured separation curves.

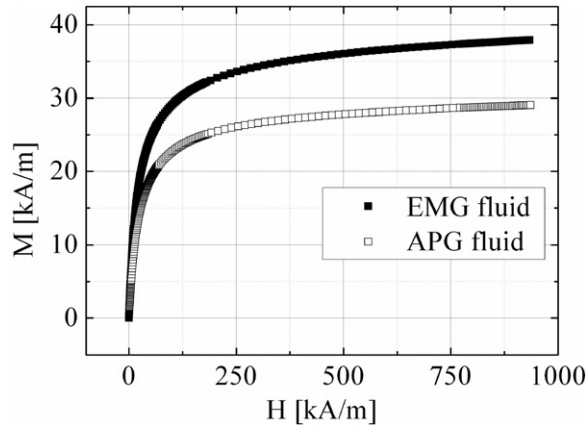


Fig. 5. Magnetisation curves of the kerosene-based EMG, and the oil-based APG fluid.

### 3.2. Fluid characterisation

Two different industrial magnetic fluids have been used for experiments, namely an EMG and an APG fluid (Ferrotec). The first one is a kerosene-based fluid, the second is oil-based, and both contain magnetite particles. The surfactant guaranteeing stability is unknown for both fluids. For the separation experiments as well as for the linear stability analysis of the thermomagnetic convection several parameters of these fluids are needed, such as volume concentration, particle diameter, viscosity, and density. Most of these parameters are provided by the magnetisation curves of the fluids, only viscosity is measured separately with an Anton Paar rheometer.

Fig. 5 shows the two magnetisation curves, determined with a LakeShore vibrating sample magnetometer (VSM) equipment. The saturation magnetisation  $M_s$  [1]

$$M_s = \phi_c M_d \quad (24)$$

gives information about the particle volume concentration  $\phi_c$  of the measured sample by knowing the saturation magnetisation of the bulk magnetite  $M_d$  [1]. The inclination of the initial linear part of the magnetisation curve, also called initial susceptibility,

$$\chi_i = \pi / 18 \phi_c \mu_0 M_d^2 d^3 / (k_B T) \quad (25)$$

provides the mean particle diameter  $d$  of the fluid [1], with  $k_B$  being the Boltzmann constant. The EMG fluid is thereby characterised by 8.67 vol% of magnetic particles of 11.6 nm in diameter referring to the magnetic core. The density is given by 1.51 g/cm<sup>3</sup>. The APG fluid is less concentrated, with 6.63 vol% magnetite particles, with a similar diameter of 11.4 nm as the particles in the EMG fluid. The density of the APG fluid can be determined to 1.44 g/cm<sup>3</sup>. Unfortunately, the mean diameter derived from the magnetisation curve does not consider the polydispersity of the particle size. Therefore a size distribution for the particles' diameter is calculated according to [16] and [17] and an average diameter, taking into account the volumetric distribution of the particles, is calculated to 10.4 nm in the case of EMG. The carrier liquid's viscosity  $\eta_{CL}$  necessary to calculate the diffusion coefficient by means of the Batchelor-corrected Einstein relation was calculated from the ferrofluids viscosity ( $\eta = \eta_{CL}(1 + 2.5\phi_c + 6.2\phi_c^2)$  [18]), which was measured for zero magnetic field with a shear-rate controlled Anton Paar rheometer. The relation reads:

$$D = (k_B T_0) / (6\pi(r + s)\eta_{CL})(1 + 1.45\phi_c) \quad (26)$$

$r + s$  denotes the sum of the particle radius and the surfactant layer thickness of 2 nm. The viscosity of the fluids for three different temperatures is shown in Fig. 6. The APG fluid with 0.173 Pa s is about one order of magnitude more viscous than the EMG fluid with 0.011 Pa s at  $T_0 = 298.15$  K. This directly affects the diffusion coefficient. For the same average temperature in the separation experiments and similar particle diameters, the coefficient of the APG fluid ( $2.6 \times 10^{-13}$  m<sup>2</sup>/s) is about one order smaller than the one of the EMG fluid ( $3.9 \times 10^{-13}$  m<sup>2</sup>/s), i.e. the APG fluid is expected to show a weaker separation signal in the separation experiments. Since the magnetic-field dependence of the diffusion coefficient cannot be determined experimentally so far, and since theoretical assumption by [11] and [19] lead to unreasonable results for the given fluid parameters, the coefficient will be held constant even under the application of a magnetic field.

### 3.3. Separation experiments

First, the experimental setup has been tested for fluid sensitivity and temperature stability. For that purpose, three different, non-magnetic, measurements have been carried out. The EMG's carrier liquid, kerosene, has been measured, to determine the temperature sensitivity of the sensor coils. In addition to that, a separation experiment has been done with

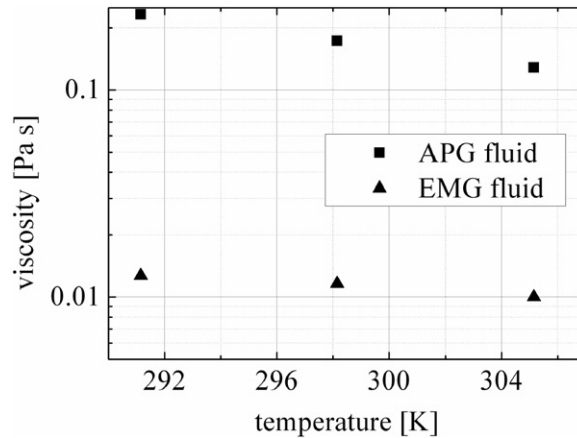


Fig. 6. Viscosity of the EMG and the APG fluid at 291.15 K, 298.15 K, and 305.15 K.

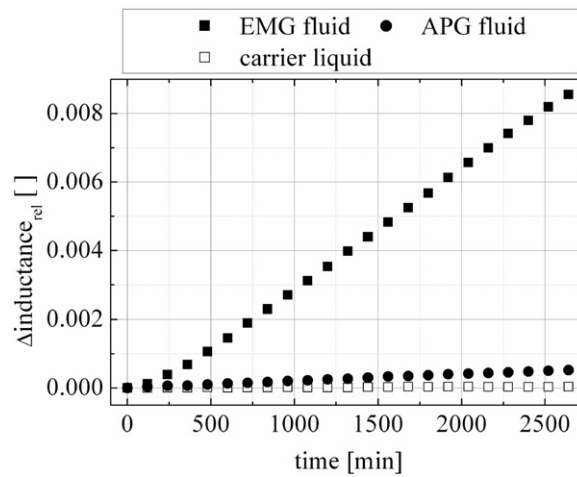
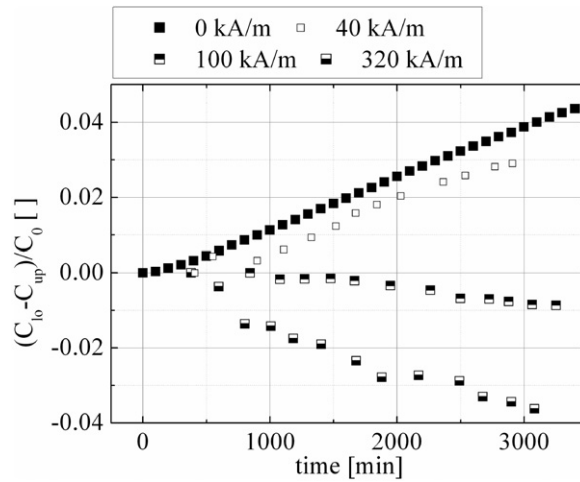


Fig. 7. Change in the difference of the relative inductance of the lower and upper sensor coil over time for kerosene, without magnetic particles, for the APG fluid with about 6.6 vol%, and the EMG fluid with about 8.7 vol% of magnetic material.

the APG and EMG fluids. All the measurements were carried out with an applied temperature gradient of 1 K/mm. In Fig. 7, the relative inductance difference of the three measurements is plotted over the separation time. For each coil the inductance is calculated normalised by the initial inductance at the beginning of the separation experiment. Then the difference of the relative inductance of the upper coil is subtracted from the one of the lower coil, which gives  $\Delta \text{inductance}_{\text{rel}}$ .

The curve for pure kerosene shows that the coils are not affected by a noticeable temperature-dependent behaviour, so that a change in the inductance is solely expected to appear due to the movement of magnetic material. The difference between the inclination of the two separation curves for the EMG and APG fluid strikes most. The signal of the EMG fluid is of one order of magnitude higher than of the APG fluid. This can be mainly explained by the different diffusion coefficients caused by a lower viscosity, resulting in a higher diffusivity of the EMG fluid. To facilitate the measurement and reduce a possible influence of the temperature, the following separation experiments for non-zero magnetic field are only carried out with the kerosene-based magnetic fluid.

The separation curves in Figs. 8 and 9 show the concentration difference of the lower and the upper fluid container normalised by the initial homogeneous concentration of the fluid over time. Applying the theoretical separation curve from Section 3.1 to the data shown, an effective Soret coefficient can be calculated using the geometry data of the measurement cell as well as the fluid parameters presented in 3.2. Fig. 10 compares the current data for the magnetic Soret coefficient with data obtained in [11]. Particularly interesting in the measurements in [11] is that a change in the sign of the Soret coefficient with increasing magnetic field strength can only be observed for parallel orientation of the magnetic field and the temperature gradient. In case of the perpendicular orientation, thermodiffusion is slightly enhanced by the magnetic field, but the particles always move to the colder side of the fluid layer, i.e. the Soret coefficient is always positive. For the fluid tested here, a change in the direction of the movement of the particles appears for both field orientations, namely between 50 kA/m and 100 kA/m, i.e. the Soret coefficient changes its sign. The separation in the perpendicular case is thereby significantly stronger, and the absolute value of the Soret coefficient is four times larger than in the parallel case.



**Fig. 8.** For the magnetic field aligned parallel to the temperature gradient, the difference in the concentration between the lower and upper fluid volume normalised by the initial homogeneous concentration is plotted. The fluid EMG is used and  $\text{grad}(T) = 1 \text{ K/mm}$ .

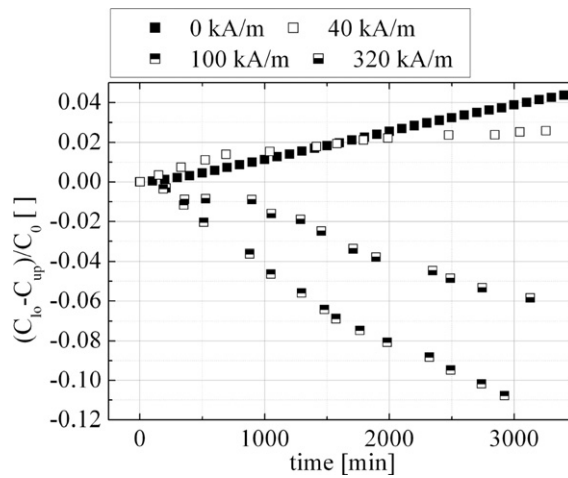


**Fig. 9.** For the magnetic field aligned perpendicular to the temperature gradient, the difference in the concentration between the lower and upper fluid volume normalised by the initial homogeneous concentration is plotted. The fluid EMG is used and  $\text{grad}(T) = 1 \text{ K/mm}$ .

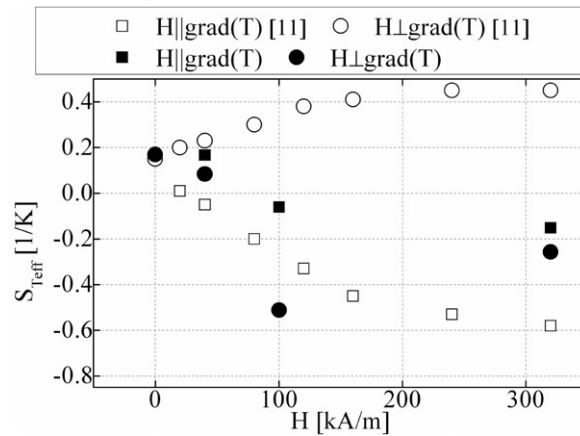


**Fig. 10.** Soret coefficient in the EMG fluid for field strengths of 0 kA/m, 40 kA/m, 100 kA/m, and 320 kA/m in both field orientations (parallel and perpendicular to the temperature gradient): full symbols; Soret coefficient for a different kerosene-based magnetic fluid for both field orientations: empty symbols [11].



#### 4. Conclusion

By means of a linear stability analysis, the behaviour of the Rayleigh number as function of the Soret coefficient could be determined. Applying free boundary conditions leads to a critical Rayleigh number of 554, neglecting thermodiffusion ( $S_T = 0 \text{ K}^{-1}$ ) and using averaged data of the magnetisation curves for the determination of the dimensionless parameters in (21). A Soret coefficient between  $-0.001 \text{ K}^{-1}$  and  $0 \text{ K}^{-1}$ , hinders the onset of convection and leads to a maximum of  $Ra_c = 1587$ . For any positive value of  $S_T$ , the convection in the layer of fluid is enhanced. Contrary a Soret coefficient being more negative than  $-0.001 \text{ K}^{-1}$  suppresses convection at all and leads to negative Rayleigh numbers.

To obtain a realistic magnitude of the Soret coefficient, magnetic-field-dependent separation experiments have been carried out with a horizontal thermodiffusion cell. The magnetic field was either applied parallel or perpendicular to the vertically oriented temperature gradient. The separation experiments in both alignments showed a diminishing Soret coefficient up to a magnetic field strength of  $75 \text{ kA/m}$ , then a change in the sign of the coefficient was detected and the value of the coefficient grew stronger negative with a further increase of the magnetic field, reaching finally  $-0.66 \text{ K}^{-1}$  at  $320 \text{ kA/m}$  in the perpendicular setup and  $-0.152 \text{ K}^{-1}$  in the parallel one.

The detection of the negative Soret coefficient combined with the analytically determined influence of the coefficient on the onset of thermomagnetic convection supports the experimentally observed dependence of the convection on the magnetic field, though comparison of the current separation data with older experiments reveals a mismatch which could be explained by the different fluids measured. Nevertheless, more and detailed investigations are necessary to solve this mismatch and to improve the understanding of thermodiffusion in magnetic fluids.

#### Acknowledgements

The authors thank Prof. Blums for very helpful discussions. Financial support by Deutsche Forschungsgemeinschaft in project LA 1182/3 is gratefully acknowledged.

#### References

- [1] R.E. Rosensweig, *Ferrohydrodynamics*, Dover Publications, Inc., Mineola, New York, 1985.
- [2] E. Blums, et al., *Magnetic Fluids*, Walter de Gruyter, Berlin, New York, 1997.
- [3] B.A. Finlayson, Convective Instability of ferromagnetic fluids, *J. Fluid Mech.* 40 (1970) 753–767.
- [4] L. Schwab, et al., Magnetic Bénard convection, *J. Magn. Magn. Mater.* 39 (1983) 113–114.
- [5] L. Schwab, et al., Thermal convection in ferrofluids under a free surface, *J. Magn. Magn. Mater.* 85 (1990) 199–202.
- [6] H. Engler, S. Odenbach, Parametric modulation of thermomagnetic convection in magnetic fluids, *J. Phys.: Condens. Matter* 20 (2008) 204135.
- [7] H. Engler, Parametric modulation of thermomagnetic convection in magnetic fluids, Thesis, 2010 (in German).
- [8] E. Blums, et al., The characteristics of mass transfer processes in magnetic fluids, *J. Magn. Magn. Mater.* 39 (1983) 142–146.
- [9] E. Blums, et al., Soret coefficient of nanoparticles in ferrofluids in the presence of a magnetic field, *Phys. Fluids* 10 (1998) 2155–2163.
- [10] T. Völker, S. Odenbach, The influence of a uniform magnetic field on the Soret coefficient of magnetic nanoparticles, *Phys. Fluids* 15 (2003) 2198–2207.
- [11] T. Völker, S. Odenbach, Thermodiffusion in ferrofluids in the presence of a magnetic field, *Phys. Fluids* 17 (2005) 037104.
- [12] S. Odenbach, T. Völker, Thermal convection in a ferrofluid supported by thermodiffusion, *J. Magn. Magn. Mater.* 289 (2005) 122–125.
- [13] S. Chandrasekhar, *Hydrodynamic and Hydromagnetic Stability*, Clarendon Press, Oxford, 1961.
- [14] A. Ryskin, et al., Thermal convection in binary fluid mixtures with a weak concentration diffusivity, but strong solutal buoyancy forces, *Phys. Rev. E* 67 (2003) 46302.
- [15] G.K. Batchelor, Brownian diffusion of particles with hydrodynamic interaction, *J. Fluid Mech.* 74 (1976) 1–29.
- [16] R.W. Chantrell, et al., Measurements of particle size distribution parameters in ferrofluids, *IEEE Trans. Magn.* 14 (1978) 975–977.
- [17] T. Weser, K. Stierstadt, Discrete particle size distribution in ferrofluids, *Z. Phys. B, Condens. Matter* 59 (1985) 253–256.
- [18] G.K. Batchelor, The effect of Brownian motion on the bulk stress in a suspension of spherical particles, *J. Fluid Mech.* 83 (1977) 97–117.
- [19] K.I. Morozov, The translational and rotational diffusion of colloidal ferroparticles, *J. Magn. Magn. Mater.* 122 (2003) 98–101.